



Direct observation of denitrogenation process of 2,3-diazabicyclo[2.2.1]hept-2-ene (DBH) derivatives, using a visible 5-fs pulse laser

Manabu Abe^{a,b,*}, Izumi Iwakura^{a,c}, Atushi Yabushita^d, Shingo Yagi^a, Jun Liu^{b,e}, Kotaro Okamura^e, Takayoshi Kobayashi^{b,d,e,f,*}

^a Department of Chemistry, Graduate School of Science, Hiroshima University, 1-3-1 Kagamiyama, Higashi-Hiroshima, Hiroshima 739-8526, Japan

^b CREST, JST, K's Gobancho, 7, Gobancho, Chiyoda-ku, Tokyo 102-0076, Japan

^c Innovative Use of Light and Materials/Life, PRESTO, JST, 4-1-8 Honcho, Kawaguchi, Saitama 332-0012, Japan

^d Department of Electrophysics, National Chiao-Tung University, 1001 Ta Hsueh Rd., Hsinchu 300, Taiwan

^e Advanced Ultrafast Laser Research Center, University of Electro-Communications, 1-5-1 Chofugaoka, Chofu, Tokyo 182-8585, Japan

^f Institute of Laser Engineering, Osaka University, 2-6 Yamada-oka, Suita, Osaka 565-0971, Japan

ARTICLE INFO

Article history:

Received 9 September 2011

In final form 7 January 2012

Available online 18 January 2012

ABSTRACT

The mechanism of denitrogenation for 2,3-diazabicyclo[2.2.1]hept-2-ene (DBH) derivatives was investigated using a visible 5-fs pulse laser. The time-dependent wavenumber changes observed in this study revealed that the concerted denitrogenation occurs in the parent DBH. However, a stepwise denitrogenation mechanism was found for the 7,7-diethoxy-substituted DBH derivative.

© 2012 Elsevier B.V. All rights reserved.

1. Introduction

The denitrogenation of azoalkanes with a functional group of $-N=N-$, such as 2,3-diazabicyclo[2.2.1]hept-2-ene derivatives (DBHs) and azobisisobutyronitrile (AIBN), is an important reaction that generates cleanly radical intermediates [1]. The reaction mechanism of the denitrogenation of DBH derivatives has been studied and discussed since 1967, when a double inversion process [2–4] was observed in the formation of 2,3-dideuterobicyclo[2.1.0]pentane during the thermal denitrogenation of *exo*-5,6-dideutero-2,3-diaza-bicyclo[2.2.1]hept-2-ene (DBH) [5–12].

Recent computational studies predicted that the denitrogenation mechanism of DBH derivatives, *concerted* versus *stepwise*, is largely dependent on the substituents X at C(7) (Scheme 1). Thus, the concerted denitrogenation process via the transition state \mathbf{TS}_c is energetically favored for the parent DBH (X = H). Meanwhile, the stepwise denitrogenation via the intermediate \mathbf{DZ} and two transition states \mathbf{TS}_{s1} and \mathbf{TS}_{s2} was found to be favored for the denitrogenation of 7,7-dialkoxy-substituted DBH derivatives (X = OR) [13,14]. The substituent effect on the denitrogenation can be rationalized by the most stable electronic-configuration of the resulting biradicals \mathbf{BR} [13]. Thus, the symmetric non-bonded molecular orbital (ψ_s) is the HOMO for the dialkoxy-substituted

biradical, for which the concerted denitrogenation is symmetry-forbidden process. The concerted denitrogenation is a symmetry-allowed process for the electron-donating substituted azoalkane such as DBH, in which the two electrons are selectively occupied in the antisymmetric non-bonded molecular orbital (ψ_a). Experimentally, the preferred mechanism of stepwise denitrogenation was suggested by the aryl-group effect on the rate constant of the denitrogenation reaction of 1,4-diaryl-7,7-dialkoxy-substituted DBH derivatives [15].

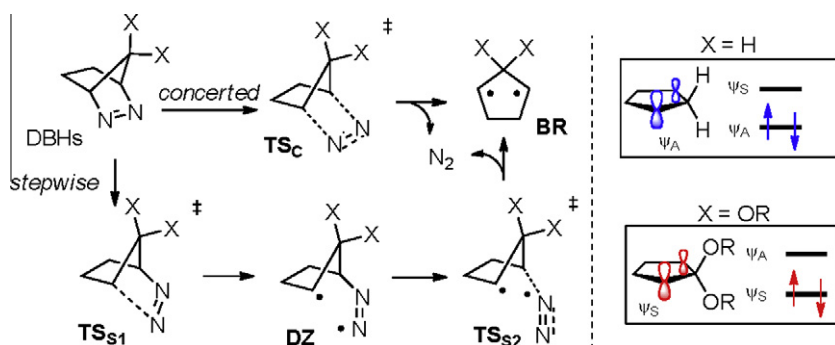
In the present study, the denitrogenation processes of 7,7-diethoxy-substituted DBH (X = OEt) and DBH (X = H) were studied using an ultrafast spectroscopy system with a visible ultra-short pulse laser developed by Kobayashi and coworkers [16,17]. Typical vibrational modes of the DBH derivatives have vibrational periods of 60–80 fs (butterfly flap mode or ring bending mode) and 20 fs (CH_2 scissoring mode). Since the pulse width of the visible pulse used in the present work was much shorter than the vibrational periods, observed signal was modulated by the molecular vibrations reflecting the real time amplitude of the modes. During chemical reactions, molecular structural changes including transition states can be traced by the time-dependent wavenumber shifts of the relevant molecular vibrational modes [18]. The direct observation of the molecular vibrational changes induced by the impulsive excitation with a visible 5-fs pulse clarified the denitrogenation processes.

2. Experimental

To obtain the visible ultrashort pulses, we have generated broadband visible light with high intensity in a non-collinear optical parametric amplifier (NOPA), and its pulse width was

* Corresponding authors at: Department of Chemistry, Graduate School of Science, Hiroshima University, 1-3-1 Kagamiyama, Higashi-Hiroshima, Hiroshima 739-8526, Japan (M. Abe), Advanced Ultrafast Laser Research Center, University of Electro-Communications, 1-5-1 Chofugaoka, Chofu, Tokyo 182-8585, Japan (T. Kobayashi).

E-mail addresses: mabe@hiroshima-u.ac.jp (M. Abe), kobayashi@ils.uec.ac.jp (T. Kobayashi).



Scheme 1. Substituent (X) effect on denitrogenation mechanism of DBH derivatives.

compressed by using a chirp mirror pair and a prism compressor, as described below.

The light source of the NOPA was a regenerative amplifier (Spectra-Physics, model Spitfire) with 150 μJ of power, a central wavelength of 790 nm, pulse duration of 100 fs, and a repetition rate of 5 kHz. The NOPA generated visible broadband extending from 525 to 725 nm. A beam splitter separated the visible broadband light pulse into two copies of the pulse to be used as a pump pulse and a probe pulse, respectively. The chirp mirror pair and the prism compressor were adjusted to compress their pulse widths as 5-fs. The polarizations of the pump and the probe pulses were parallel to each other. The focal spot areas of the pump and the probe pulses were 100 and 75 μm^2 , respectively. The probe pulse was dispersed using a polychromator (300 grooves/mm, 500 nm blazed). A 128-channel fiber bundle sends each spectral component of the dispersed probe pulse to each piece of 128 avalanche photodiodes simultaneously. The time-resolved difference transmittance, ΔT , was measured simultaneously by avalanche photodiodes in the range of 525–725 nm. The signal-to-noise ratio was improved by coupling the signals of avalanche photo-diodes to a 128-channel lock-in amplifier.

A neat liquid sample of 7,7-diethoxy-substituted DBH derivative [19] and a CH_2Cl_2 solution sample of DBH [20] (100 mg/100 μl) were prepared for a pump–probe measurement. Because DBH is a solid sample, the solvent is needed to make a solution. In order to avoid the solvent effect on changing the denitrogenation mechanism, aprotic and non-polar solvent, i.e. CH_2Cl_2 , was used for the experiment. A liquid cell with an optical path length of 1 mm was used to contain the sample. All measurements were performed at room temperature.

3. Results and discussion

3.1. Pump–probe experimental results

The azo-chromophore ($-\text{N}=\text{N}-$) of DBH derivatives has an absorption band at around 350 nm (Figure 1a). This clearly indicates that the photodenitrogenation of the DBH derivative does not occur under the conditions of one-photon absorption of the visible 5-fs pulse laser (Figure 1b). The ultrashort visible pulse excites vibration modes coherently in the electronic ground state through the stimulated Raman process, which triggers reaction in the electronic ground state like the thermal excitation by heating [21–23].

Pump–probe measurements were performed for the 7,7-diethoxy DBH derivative and the parent DBH. Figure 2 shows two-dimensional displays of absorbance changes (ΔA) in the probe delay time from -200 to 2900 fs following the visible 5-fs pulse excitation of the two DBH derivatives. The signal of ΔA was calculated as $\Delta A = -\log_{10}(1 + \Delta T/T)$, where T and ΔT are the transmittance

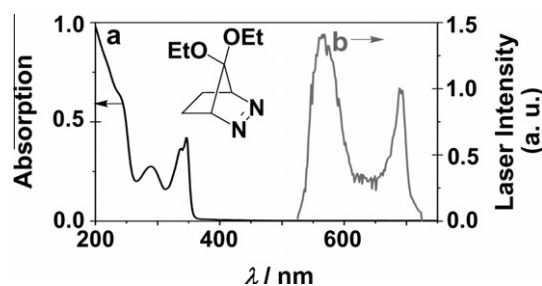


Figure 1. (a) Absorption spectrum of 7,7-diethoxy-substituted DBH derivative (black curves) and (b) the visible 5-fs pulse laser (gray curves) spectra.

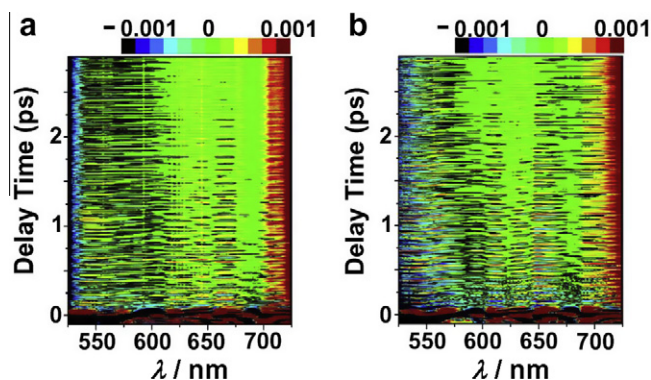


Figure 2. Two-dimensional displays of the absorbance changes plotted two-dimensionally against the probe delay time and the wavelength following the visible 5-fs pulse excitation of (a) the 7,7-diethoxy-substituted DBH derivative and (b) DBH.

and the transmittance change, respectively, induced by the pump pulse. The absorbance change was oscillating around zero, which indicates that the signal modulation is not due to the population dynamics of the electronic excited states. The Fourier power spectra were obtained from the real-time traces from 200 to 800 fs (Figure 3a and b). The wavenumber resolution of Fourier power spectrum was estimated to be 16 cm^{-1} .

The wavenumber modes observed in Figure 3a reflect the vibrational modes of the 7,7-diethoxy DBH derivative. The wavenumber modes were assigned to the butterfly flap modes (325 and 480 cm^{-1}), the ring bending mode (δ_{Ring} : 887 cm^{-1}), the CH_2 wagging mode (δ_{CH_2} : 976 cm^{-1}), and the CH deformation mode (δ_{CH} : 1139 cm^{-1}), whose assignments were done on the basis of the reported assignments for DBH [24] and frequency calculations [25]. The wavenumber modes around 285 and 700 cm^{-1} in Figure 3b, for DBH solution in CH_2Cl_2 , were assigned to the C–Cl scissoring

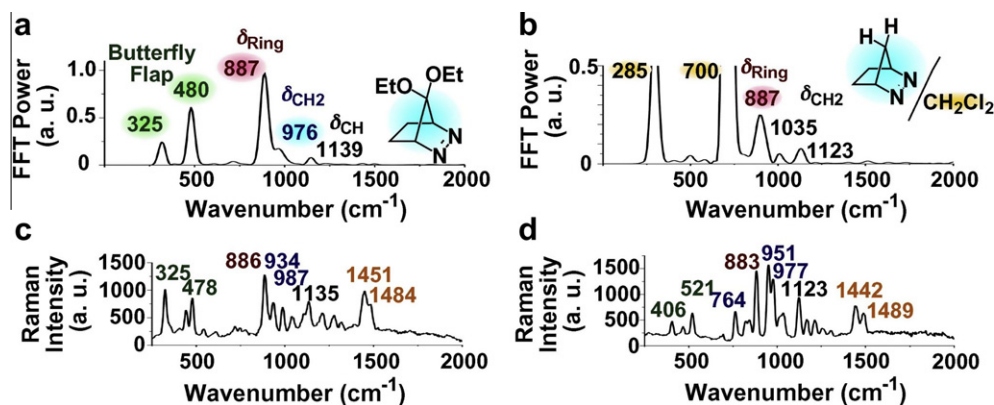


Figure 3. Fourier power spectra of the real-time trace from 200 to 800 fs of (a) the 7,7-diethoxy-substituted DBH and (b) DBH. Raman spectra of (c) the 7,7-diethoxy-substituted DBH and (d) DBH.

mode (δ_{C-Cl}) and to the C–Cl stretching mode (ν_{C-Cl}) in the CH_2Cl_2 solvent molecule. The other observed frequencies shown in Figure 3b can be assigned to the ring-bending mode (δ_{Ring} : 887 cm^{-1}), to the CH_2 wagging mode (δ_{CH_2} : 1035 cm^{-1}), and to the CH deformation mode (δ_{CH} : 1123 cm^{-1}) [24]. The frequencies observed by the pump–probe measurements (Figure 3a and b) agreed well with the respective ground-state Raman frequencies (Figure 3c and d). Since the pump laser is not resonant with the electronic transition in the DBH molecule, the observed modulation of ΔT is due to the wavepacket in the ground state. Hence the frequencies of the FT of the real-time traces are expected to agree with the Raman wavenumber in the electronic ground state. The pump–probe spectroscopy and Raman measurement are members of a broad class of nonlinear optical techniques related to the third-order optical polarization and the corresponding susceptibility. Therefore, the pump–probe signal shows Raman active

modes. However, the two methods differ by their measurement mechanism, which results in difference in the signal intensities.

The Fourier phases of the real-time traces showed that the observed molecular vibrations follow a sine-like oscillation, which confirmed that the observed signals reflect the wavepacket dynamics in the electronic ground state (Figure 4a and b). The pump intensity dependence of the vibrational amplitudes also supports assignment of the observed oscillating signal to the ground state, as described below. Three sets of measurements were performed maintaining the probe intensity at 20 GW cm^{-2} (Figure 4c and d). In the case of the 7,7-diethoxy DBH derivative ($X = OEt$) with pump intensities of 120, 135, and 160 GW cm^{-2} , the powers $p(i)$ of the pump intensity dependence $p^{(i)}$ for three modes (325 , 887 , and 976 cm^{-1}) were determined to be $p(325\text{ cm}^{-1}) = 1.1 \pm 0.1$, $p(887\text{ cm}^{-1}) = 0.9 \pm 0.1$, and $p(976\text{ cm}^{-1}) = 1.2 \pm 0.7$ (Figure 4c). In the case of DBH with pump intensities of 105, 123, and

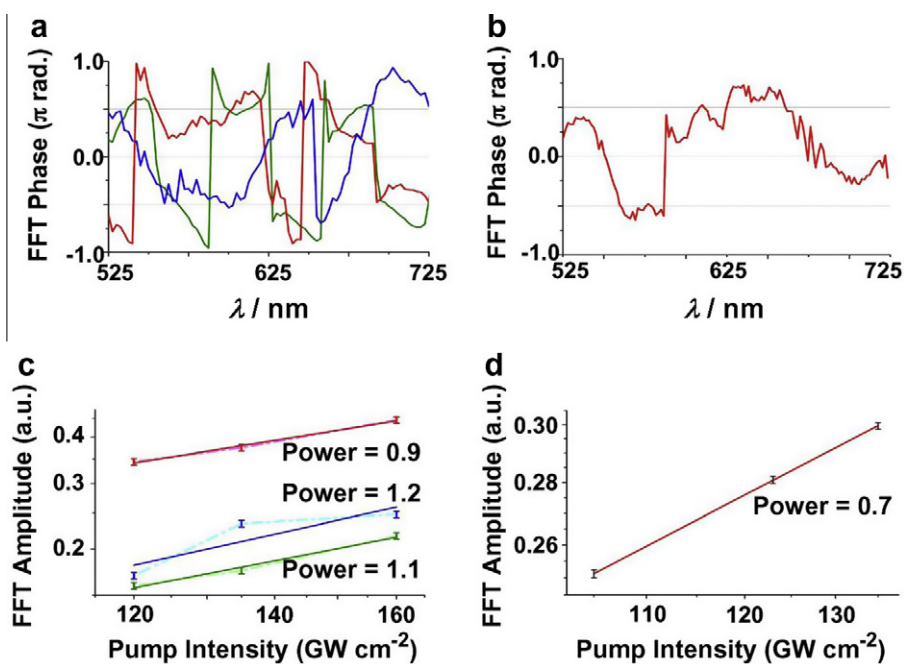


Figure 4. Fourier phase spectra of the observed molecular vibrations of (a) the 7,7-diethoxy-substituted DBH with frequencies of 325 cm^{-1} (green curve), 887 cm^{-1} (red curve), and 976 cm^{-1} (blue curves) and (b) DBH with wavenumber of 887 cm^{-1} (red curve). Pump intensity dependencies of vibrational amplitudes the same condition of the probe intensity of 20 GW cm^{-2} are shown for (c) the 7,7-diethoxy-substituted DBH with frequencies of 325 cm^{-1} (green curve and green crosses), 887 cm^{-1} (red curve and red crosses), and 976 cm^{-1} (blue curve and blue crosses) and (d) DBH with wavenumber of 887 cm^{-1} (red curve and red crosses).

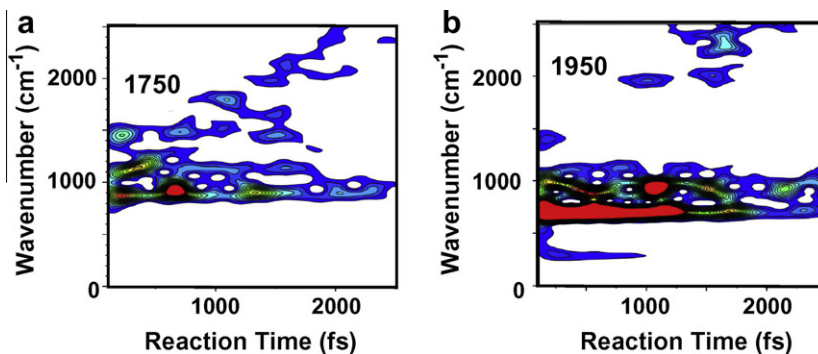
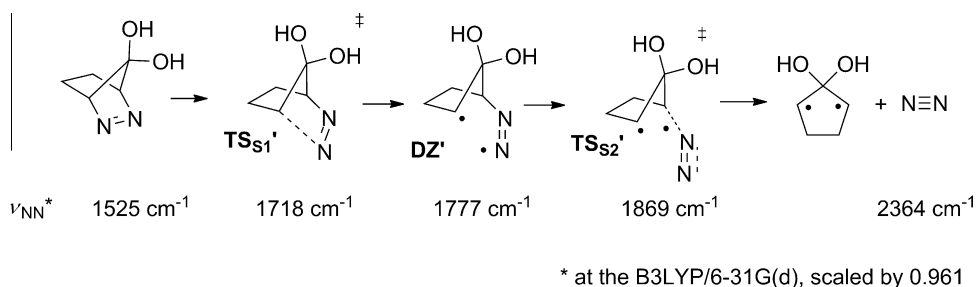


Figure 5. Spectrograms of (a) the 7,7-diethoxy-substituted DBH derivative and (b) DBH.



Scheme 2. Wavenumber change of DBH derivative (X = OH) during the stepwise denitrogenation, see Ref. [25].

135 GW cm^{-2} , the power of the pump intensity dependence of the vibrational amplitude was determined to be $p(887 \text{ cm}^{-1}) = 0.70 \pm 0.01$ (Figure 4d). The linear pump intensity dependence suggests that the observed oscillation of ΔA is not due to the dynamics of the electronic excited state generated by multi-photon absorption, but is predominantly due to the wave-packet generated in the ground state through the stimulated Raman process.

3.2. Spectrogram

The time-dependent wavenumber shifts of the relevant molecular vibrational modes were analyzed using Spectrograms, which have been used for time-resolved analysis of Fourier power spectra. Spectrograms [26] shown in Figure 5 were calculated by applying a sliding-window Fourier transform to the ΔA traces averaged over 10 probe wavelengths. A Blackman window function with a full width half maximum of 240 fs was used for the spectrograms, as shown in Eq. (1). The spectrogram trace was calculated by shifting the window at 10-fs step in the delay time.

$$S(\omega, \tau) = \int_0^\infty S(t)g(t - \tau) \exp(-i\omega t) dt, g(t) = 0.42 - 0.5 \cos 2\pi t + 0.08 \cos 4\pi t \quad (1)$$

The wavenumber resolution of the spectrogram is 30 cm^{-1} . The data in the vicinity of a zero delay was disturbed by the interference between the scattered pump and the probe pulses. Molecular structure deformation during the reaction process along the reaction coordinate changes the oscillation wavenumber of the wave packet oscillating along the coordinate perpendicular to the reaction coordinate. The transfer of vibrational coherence, or even the generation of coherence, in chemical reaction was previously discussed and demonstrated [27–31]. When the molecule stays either in the reactant, the intermediate, or the product, the vibration frequencies are thought to be constant during the lifetime of the

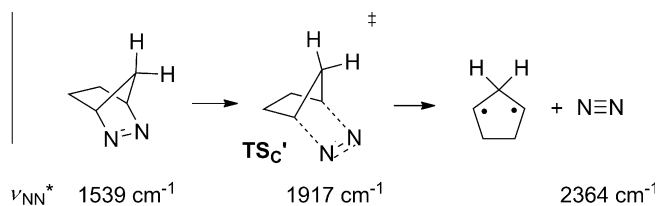
relevant state although the vibration frequencies might be different between those electronic states. The vibrational frequencies are considered to change gradually when the molecule undergoes the structural change from the reactant, through the intermediate, and finally to the product.

In the reaction of 7,7-diethoxy DBH derivative (Figure 5a), vibrational bands appeared around 900, 1050, and 1450 cm^{-1} just after the photo-excitation. These modes can be assigned to the ring bending modes, the CH_2 wagging mode, and the CH_2 scissoring mode, respectively. The CH_2 wagging mode started to blue-shift after photo-excitation, and two new bands appeared at around 1300 and 1750 cm^{-1} at ca. 1 ps after the photo-excitation, which are assigned to the CH bending mode and NN stretching mode, respectively.

Meanwhile, just after photo-excitation of DBH (Figure 5b), the CH_2 bending modes appeared at around 1000 and 1450 cm^{-1} and vibrational modes of the CH_2Cl_2 solvent appeared at around 300 and 700 cm^{-1} . At ca. 1 ps after the photo-excitation, a vibrational band appeared at around 1950 cm^{-1} being assigned to the NN stretching mode, which has higher wavenumber than that observed for the 7,7-diethoxy-substituted DBH (1750 cm^{-1}).

3.3. Denitrogenation mechanism

As mentioned in the Introduction (Scheme 1), two possible mechanisms, either the concerted pathway or the stepwise pathway [1–14], can be considered to understand the dynamics observed in the denitrogenation of DBH derivatives. The electron density of the NN bond is supposed to be higher in the transition state (TSC) of the concerted process than those in the intermediate (DZ) and the transition states (TS_{S1} and TS_{S2}) for the stepwise process (Scheme 1). Thus, the NN stretching vibrational mode of TSC should have higher wavenumber than those in DZ, TS_{S1} , and TS_{S2} . Indeed, it was also predicted by a theoretical calculation performed at the (U)B3LYP/6-31G(d) level showing that the NN stretching



* at the B3LYP/6-31G(d), scaled by 0.961

Scheme 3. Wavenumber change of DBH (X = H) during the concerted denitrogenation, see Ref. [25].

modes (ν_{NN} , scaled by 0.961) of the model intermediary species $\text{TS}_{\text{S}1}$ ($\nu_{\text{NN}} = 1718 \text{ cm}^{-1}$, imaginary wavenumber (ν^i) = -240 cm^{-1}), DZ' ($\nu_{\text{NN}} = 1777 \text{ cm}^{-1}$), and $\text{TS}_{\text{S}2}$ ($\nu_{\text{NN}} = 1869 \text{ cm}^{-1}$, imaginary wavenumber (ν^i) = -405 cm^{-1}) have lower wavenumber than that of the transition state TS_{C} ($\nu_{\text{NN}} = 1917 \text{ cm}^{-1}$, imaginary wavenumber (ν^i) = -492 cm^{-1}) (see Schemes 2 and 3) [13,25].

Spectrogram analysis of the measured time-resolved traces found large wavenumber difference in the NN stretching mode at a 1 ps delay between the 7,7-diethoxy DBH derivative and the parent DBH, i.e. 1750 cm^{-1} in Figure 5a and 1950 cm^{-1} in Figure 5b. Considering above prediction given by the theoretical calculation, the observed wavenumber difference elucidates that the denitrogenation of the 7,7-diethoxy DBH derivative proceeds through the stepwise pathway, and that of the parent DBH proceeds through the concerted pathway. After a 1 ps delay, the NN stretching frequencies increased with a delay in both of the compounds, reflecting the dissociation of nitrogen. The observed blue shift of the NN stretching wavenumber also agrees with the computational prediction.

4. Conclusion

In summary, the reaction mechanism of the thermal denitrogenation of DBH derivatives was investigated using a visible 5-fs pulse laser, by which the time-dependent wavenumber shift of molecular vibrations is directly observed. The concerted denitrogenation process was found in the thermolysis of the parent DBH. However, the stepwise nitrogen dissociation process was observed for the denitrogenation of the 7,7-diethoxy DBH derivative. These results agree well with the computational predictions. The ultrashort visible pulse excited vibrational modes coherently in the electronic ground state through the stimulated Raman processes, which precedes the reaction in the electronic ground state like the thermal excitation under heating.

Acknowledgments

NMR and MS measurements were made using JEOL JMN-LA500 and Thermo Fisher Scientific LTD Orbitrap XL spectrometers, respectively, at the Natural Science Center for Basic Research and Development (N-BARD), Hiroshima University. M. A. acknowledges financial support in the form of a Grant-in-Aid for Scientific Research on Innovative Areas 'π-Space' (No 21108516), the Scientific Research (No. 19350021), Tokuyama Science Foundation, and Mazda Foundation. A. Y. acknowledges financial support in the National Science Council of the Republic of China, Taiwan (Grant No. NSC 98-2112-M-009-001-MY3, Grand No. NSC 99-2923-M-009-004-MY3). T. K. acknowledges financial support in a grant from the Ministry of Education in Taiwan under the ATU Program at National Chiao Tung University.

References

- [1] P.S. Engel, Chem. Rev. 80 (1980) 99.
- [2] W.R. Roth, M. Martin, Liebigs Ann. Chem. 702 (1967) 1.
- [3] W.R. Roth, M. Martin, Tetrahedron Lett. (1967) 4695.
- [4] E.L. Allred, R.L. Smith, J. Am. Chem. Soc. 91 (1969) 6766.
- [5] W. Adam, H. Garca, V. Marti, J.N. Moorthy, J. Am. Chem. Soc. 121 (1999) 9475.
- [6] W. Adam, M. Diedering, A. Trofimov, J. Phys. Org. Chem. 17 (2004) 643.
- [7] W. Adam, T. Oppenlaender, G. Zang, J. Org. Chem. 50 (1985) 3303.
- [8] N. Yamamoto, M. Olivucci, P. Celani, F. Bernardi, M.A. Robb, J. Am. Chem. Soc. 120 (1998) 2391.
- [9] A. Sinicropi, C.S. Page, W. Adam, M. Olivucci, J. Am. Chem. Soc. 125 (2003) 10947.
- [10] B.A. Lyons, J. Pfeifer, T.H. Peterson, B.K. Carpenter, J. Am. Chem. Soc. 115 (1993) 2427.
- [11] M.B. Reyes, B.K. Carpenter, J. Am. Chem. Soc. 120 (1998) 1641.
- [12] M.B. Reyes, B.K. Carpenter, J. Am. Chem. Soc. 122 (2000) 10163.
- [13] M. Abe, C. Ishihara, S. Kwanami, A. Masuyama, J. Am. Chem. Soc. 127 (2005) 10.
- [14] M. Hamaguchi, M. Nakaishi, T. Nagai, T. Nakamura, M. Abe, J. Am. Chem. Soc. 129 (2007) 12981.
- [15] C. Ishihara, M. Abe, Aust. J. Chem. 63 (2010) 1615.
- [16] A. Baltuska, T. Fuji, T. Kobayashi, Opt. Lett. 27 (2002) 306.
- [17] T. Kobayashi, A. Shirakawa, T. Fuji, IEEE J. Quant. Electron. 7 (2001) 525.
- [18] T. Kobayashi, T. Saito, H. Ohtani, Nature 414 (2001) 531.
- [19] S.L. Buchwalter, G.L. Closs, J. Am. Chem. Soc. 131 (1979) 4688.
- [20] P.G. Gassman, K.T. Mansfield, Org. Synth. 49 (1969) 1.
- [21] I. Iwakura, A. Yabushita, T. Kobayashi, J. Am. Chem. Soc. 131 (2009) 688.
- [22] I. Iwakura, A. Yabushita, T. Kobayashi, Chem. Lett. 39 (2010) 374.
- [23] I. Iwakura, A. Yabushita, T. Kobayashi, Chem. Phys. Lett. 501 (2011) 567.
- [24] D. Gernet, W. Kiefer, Fresenius J. Anal. Chem. 362 (1998) 84.
- [25] S. Yagi, Y. Hiraga, R. Takagi, M. Abe, J. Phys. Org. Chem. 24 (2011) 894.
- [26] M.J.J. Vrakking, D.M. Villeneuve, A. Stolow, Phys. Rev. A 54 (1996) R37.
- [27] J.M. Jean, G.R. Fleming, J. Chem. Phys. 103 (1995) 2092.
- [28] F. Rosca, A.T.N. Kumar, X. Ye, T. Sjodin, A.A. Demidov, P.M. Champion, J. Phys. Chem. A 104 (2000) 4280.
- [29] M.H. Vos, F. Rappaport, J.-C. Lambry, J. Breton, J.-L. Martin, Nature 363 (1993) 320.
- [30] R.J. Stsnley, S.G. Boxer, J. Phys. Chem. 99 (1995) 859.
- [31] Q. Wang, R.W. Schoenlein, L.A. Peteanu, R.A. Mathies, C.V. Shank, Science 266 (1994) 422.